Nano Communication Networks 2 (2011) 213–222

Contents lists available at SciVerse ScienceDirect

Nano Communication Networks

journal homepage: www.elsevier.com/locate/nanocomnet

Modeling signal propagation in nanomachine-to-neuron communications

Laura Galluccio *, Sergio Palazzo, G. Enrico Santagati

Dipartimento di Ingegneria Elettrica, Elettronica ed Informatica, Università degli Studi di Catania, Italy

ARTICLE INFO

Article history:
Received 15 August 2011
Accepted 19 August 2011
Available online 13 October 2011

Keywords:
Nanonetworks
Nanomachines
Neuronal communications
Signal propagation
Modeling

ABSTRACT

Nanomachine communications are a promising paradigm for the large applications which can be envisaged especially in the medical field. As an example, many widespread neurological diseases such as Alzheimer and/or paralysis are associated to bad neuronal communication or to interruption of the pulse propagation across the nervous system due to irreversible damages across a human body area. In this context, nanomachines can be integrated into a neuronal network system to restore biological communications. To this purpose, a preliminary step is modeling all the phases of the communication among neurons through a block scheme where input/output relationships at each block are characterized in terms of transfer functions, gain and delay. In order to make the characterization realistic, we also consider the possibility to have multiple inputs along the surface of a neuron cell. The communication perspective being used can be useful to design nanomachines compatible with biological structures and able to interact with biological systems.

1. Introduction

Nanonetworking is a futuristic but very promising research field which is expected to provide significant benefits to the scientific and medical community in the next decade. The potentialities are huge, especially in terms of replacement or recovery of biological entities. As an example, it is well known that some neurological diseases, such as Alzheimer, are due to erroneous patterns originated by misfunctioning neuronal communications. Also in the case of severe accidents, the irreversible damage to a part of the spinal cord makes propagation of nervous pulses impossible, thus causing the paralysis of an individual.

To cope with these impairments, nanonetworks composed of nanomachines can be expected to partially replace the damaged/misfunctioning segments of the nervous system provided they exactly behave like biological entities, so that nervous pulse propagation can be supported. To this purpose, neuronal communication should be modeled in detail so that each composing module can be reproduced.

However, when talking about nanonetworking, not only models for application to neuronal networks have been discussed; actually, various other communication paradigms have been introduced in the last years. Basically, two classes of paradigms have been adopted: purely molecular and electromagnetic. *Molecular communications* [12] exploit chemical diffusion of particles and molecules as in living organisms while also performing coding and information transmission through chemical features. Different molecular communication ranges can be considered, as proposed in [1,11]: short range communications (few nm to μm), where calcium signaling [18] or molecular motors [17] can be used to propagate information; medium range communications (μm to mm), where flagellated bacteria and catalytic nanomotors have been proposed as carriers [11]; long range communications (few mm) where pheromones, pollens and spores, as well as neurons, have also been considered but no specific physical models have been proposed so far [19]. *Electromagnetic communications*, on the other hand, rely on the use of appropriate transmitters and receivers [13,23] as well as

* Corresponding author.
E-mail address: lauragalluccio@gmail.com (L. Galluccio).

1878-7789/$ – see front matter © 2011 Elsevier Ltd. All rights reserved.
doi:10.1016/j.nancom.2011.08.002

exploitation of carbon nanotube antennas [14,16,2] which are currently at an initial design stage. Also in this case much attention has been devoted to design RF circuitry to support such kind of communications and explore channel capacity [15].

In a previous paper [9] we dealt with molecular communications and, in particular, we focused on long range communications as supported by neurons in their interaction. To this purpose we provided a system description of signal propagation in nanomachine-to-neuron communications, where however a neuron has been considered as an isolated entity with no simultaneous interactions with other neurons.

Differently from our previous work, in this paper we perform a realistic analysis where the possibility that multiple inputs are applied to each neuron is also considered, as it actually happens when a neuron is regarded as a part of a more complex neuronal network. All the phases of neuronal processing are described in terms of input/output relationship, i.e. transfer functions for each functional block being identified. Gain and delay introduced by each block are modeled and the overall system characterized in terms of an end-to-end transfer function which depends on the operating frequency.

The rest of this paper is organized as follows. In Section 2 we describe the neuron structure. In Section 3 we provide a mathematical characterization of signal propagation in neuronal systems, which is then used in Section 4 to investigate on the neuronal system frequency behavior. Finally, in Section 5, concluding remarks are drawn.

2. Fundamentals of neuron structure

In this section we describe some basic concepts on how signals are transmitted in a biological nervous communication system.

The nervous system is organized as a network of neurons. Each neuron receives inputs by a certain number N of other neurons and provides output to other M neurons.[1] To this purpose, it is composed of *dendrites*, having a tree structure, which can be identified with the input interface, an *axon* used as the output interface, and a cell body, called *soma*, which implements the system logic.[2]

The axon arises from the cell soma at the *axon hillock* characterized by a high concentration of ions channels. External signals reach the dendrites, propagate through the soma, and, once in the axon hillock, depending on the strength, can generate an *Action Potential* propagated throughout the axon till the *axon terminal button*, where the *synapse*, i.e. a junction, allows signal propagation to other cells.[3] The axon can be up to one meter long (e.g. in the ischiatic nerve of human beings) and can be wrapped up by a *myelin sheath* used to shield the signal and allow propagation on a longer range; alternatively, the axon could also be unshielded and not wrapped by the myelin sheath. In case of nerve fibers, axon is always myelined to guarantee higher propagation speed and lower energy consumption. Observe that, due to the possible significant axon length, a high attenuation of the action potential while traveling along it could be met. To decrease the impact of channel attenuation in the axon, the myelin sheath is interrupted at some gap locations along the axon called *Ranvier nodes*. The typical size of these interruptions is around 1 μm. Ranvier nodes are locations where electrical signals can be regenerated due to the high concentration of voltage-gated ion channels. Action potential is regenerated at these sites so that it finally comes at the axon terminal button. The result of the regeneration of the action potential at the Ranvier nodes is the, so called, *saltatory conduction*. Once the action potential reaches the axon button terminal it leads to neurotransmitters' emission across the *synapse* which is the junction between a pair of neurons. At the postsynaptic element, binding between neurotransmitters and receptors implies generation of a synaptic current and, again, propagation of the action potential through a different neuron. The scheme of a generic neuron is shown in Fig. 1.

In this paper we characterize how signals propagate from dendrites (i.e. input interface of the neuron) to the axon terminal button (output interface of the neuron); however, before describing such a system, we need to introduce some basics on general cellular structure.

2.1. Cellular membrane

The cellular membrane is a fundamental element of all cells, including neurons. The membrane separates the internal cytoplasm from the extracellular medium.

Distribution of ions[4] in a cell is not at an equilibrium; in fact, there always exists an ion gradient which causes a diffusion process across the cellular membrane; this is fundamental for cells' activity. As an example consider that typically there is an excess of sodium and chlorine ions Na^+ and Cl^- outside, and potassium ions K^+ inside. This difference in ions' concentration induces a voltage difference also when the cell is not hit by any stimulus. This voltage difference is called *resting potential*. The ion gradient is maintained through an active transport system which continuously contrasts passive diffusion due to chemical equilibrium. Existence of stable ion gradient between the internal and external parts of a cell leads to a variation in membrane electrical potential. Membrane potential is the triggering element during nervous excitement since it allows the generation of electrical signals needed by neuronal communication. It is possible to efficiently modulate the membrane potential amplitude simply varying the membrane permeability to specific ions.

[1] Observe that, in general, neurons can receive input from and provide output to other cells besides neurons. We here do not consider this to keep our discussion easier.

[2] There are different specialized types of neurons which can have slightly different structures but, in the rest of this paper, we will refer to the generic structure mentioned above.

[3] Actually two types of synapses exist: electrical (rarely) and chemical (more commonly). In the rest of this paper we will focus only on chemical synapses since they are the most widespread in biological creatures.

[4] Ions are electrically charged particles.

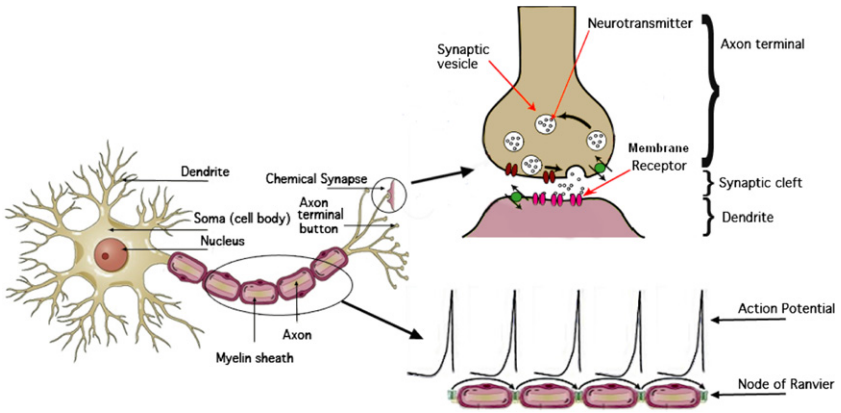

Fig. 1. Neuron model.

Cell membrane consists of a phospholipid bilayer with embedded proteins able to perform basic functionalities for cell activity. The main membrane proteins can be classified as *Membrane receptors*, *Ion channels* and *Ion pumps*. *Membrane receptors* can bind only to certain molecules, called *ligands*, thus causing the activation of a specific biological or chemical effect. The membrane receptors involved in neuronal communications are placed in the dendrites and bind to certain proteins (the ligands) called neurotransmitters which are released in the synapse by the axon terminal button of a previous neuron.

Ion channels form aqueous pores in the phospholipid bilayer which allow ions' exchange through membrane. Obviously the voltage difference at the cellular membrane can be modulated by varying the number of open ion channels on the following of the binding between the receptors and the neurotransmitters due to the propagation of an action potential.

Ion pumps carry ions against their gradient using energy from ATP (Adenosine Triphosphate) hydrolysis and allow *membrane active transport* to maintain voltage difference at the cellular membrane.

2.2. Action Potential

When neurons are stimulated by external sources (e.g. during neuronal excitation), basically two types of responses take place: passive and active. Experimental tests show that, if electrical current flows through the cell membrane, this reacts passively like a RC parallel circuit where R is the resistive component of ions' transportation through ion channels at the membrane, and C represents the membrane capacitive component associated to the dielectric properties of the phospholipid bilayer.

In addition to a passive response, an excitable cell also exhibits an active response, called *Action Potential* or *spike*. If external stimulus is strong enough to make the membrane potential rise up to a threshold value, a depolarization occurs, and the response activates an *all-or-none* event in which the electrical membrane potential of a cell rapidly rises and then falls. The reason for this behavior is that when the sodium channels are open, they allow an incoming flow of sodium ions, which changes the electrochemical gradient; this in turn leads to a depolarization in the membrane potential which causes more sodium channels to open, producing a larger electric current. The process goes on until all the available sodium channels are open, causing a rise in the membrane potential. Due to the incoming flux of sodium ions, the membrane reverses its polarity and the sodium channels then rapidly inactivate. When the sodium channels close, ions can no longer enter the neuron and are left out of the membrane. Potassium channels are then activated so reporting the electrochemical gradient to the initial resting state.

The Action Potential cannot be reinvoked immediately but there is an Absolute Refractory Period (ARP) that must elapse before a new Action Potential can be invoked due to the reactivation time in the ion channels.

2.3. Synaptic transmission

Transmission of electrical signals between excitable cells (e.g. neurons) takes place in specialized sites called *synapses*. Transmitter and receiver cells are defined as *presynaptic* and *postsynaptic* cells. Space between the two parts is called *synaptic cleft*. According to the communication strategy being used, we can classify synapse into electrical and chemical. The former allows direct communication between presynaptic and postsynaptic cells using electrical signals. The latter leads to a double signal transduction during transmission. Action potential generated by a presynaptic cell is transduced into a chemical signal, i.e. neurotransmitter concentration, which, once reaches the postsynaptic cell, is re-transduced into a membrane potential.

Neurotransmitters' release in the synaptic cleft is caused by the Action Potential generated at the presynaptic cell, which forces neurotransmitter exocytosis from special containers called *synaptic vesicles* (see Fig. 1).

3. Model

Our objective is to model signal propagation between two neurons. This communication system can be represented as shown in Fig. 2. In this figure two entities are depicted, TX and RX. In the rest of this paper we will model the blocks inside the dotted line which correspond to the

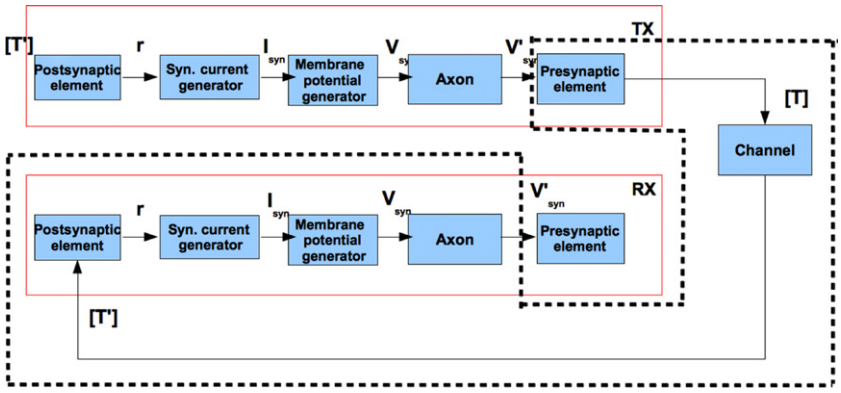

Fig. 2. System building blocks.

condition when the signal enters the presynaptic element of the TX and then leaves the axon of the RX.

As depicted in the scheme, this communication system can be considered as composed of different blocks; each of them properly models a phase in neuronal communication. In the following we will analyze in detail each block, describing how it works and how it is characterized in term of input/output relationship, gain and delay.

3.1. Presynaptic element

The first block represents the presynaptic element of a chemical synapse. An information transduction is required in order to obtain a chemical signal from an electrical one. In detail, this block accepts as input a voltage value v and returns as output the concentration of neurotransmitters currently released T. We assume that the input/output relationship follows a Boltzmann distribution as in [8]

$$T(v) = T_M / \left[1 + e^{-\frac{v - V_p}{k_p}}\right] \tag{1}$$

where T_M is the maximum neurotransmitters' concentration that can be released, v is the presynaptic voltage or action potential at TX (i.e. input signal), V_p is called the half-activation potential and k_p is a slope factor.

Observe that, as suggested by experimental observations, due to the action potential mechanism, the neurotransmitters' concentration in the time domain typically exhibits an impulsive rectangular behavior and can be modeled as [3]

$$T(t) = T_M \cdot [u(t - t_0) - u(t - t_1)] \tag{2}$$

where $u(\cdot)$ is the Heaviside step function, and t_0 and t_1 are the time instants when the neurotransmitters' release starts and ends.

Observe that, in the frequency domain, by using the Fourier transform [4], the normalized concentration of neurotransmitters can be modeled as

$$T(f) = \mathrm{sinc}(f(t_1 - t_0))e^{-j2\pi f(t_1 - t_0)}. \tag{3}$$

Accordingly the gain of the first block is

$$H_1(f) = \frac{T(f)}{V_{syn(f)}} \tag{4}$$

and the associated delay can be calculated as

$$D_{H_1}(f) = -d\phi_{H_1}/df = -d\left(\arctan\left(\frac{\Im(H_1(f))}{\Re(H_1(f))}\right)\right)/df. \tag{5}$$

This output concentration is propagated through the synaptic cleft. Accordingly, a variation in the neurotransmitters concentration occurs as a function of the distance traveled in the cleft. In the following section, this diffusion through the synaptic cleft will be characterized.

3.2. Channel

Usually the diffusion of the neurotransmitters across the synaptic cleft is not modeled [8] and the synaptic cleft is considered as a reliable channel which does neither attenuate nor introduce any delay in the signal propagation. Instead, an accurate characterization of signal propagation requires to consider also the neurotransmitters diffusion in the cleft. Accordingly, in this section, we recall the main aspects of the particle diffusion process described in [20] to model this propagation of neurotransmitters through a diffusive approach.

Let us consider a concentration T of neurotransmitters which travel through the synaptic cleft, which size is d_{Cleft}. By using the diffusion theory [22], and, in particular, the second Fick's law and the Telegraph equation [22], the concentration variation inside the cleft can be modeled using a normalized gain function as [20]

$$\frac{T'(f)}{T(f)} = H_2(f) = \frac{\int_{-\infty}^{+\infty} g(d_{Cleft}, t)e^{-j2\pi ft}dt}{\max_f\left(\int_{-\infty}^{+\infty} g(d_{Cleft}, t)e^{-j2\pi ft}dt\right)} \tag{6}$$

where $T'(f)$ is the concentration of neurotransmitters at the postsynaptic element, and $g(\cdot)$ is the impulse response of the system and can be written as [20]

$$g(d_{Cleft}, t) = e^{-t/(2\tau)}\frac{\cosh\left(\sqrt{t^2 - (\|x\|/c)^2}\right)}{\sqrt{t^2 - (\|x\|/c)^2}} \cdot u(t - \|x\|/c) \tag{7}$$

being $\|x\|$ the distance from the presynaptic terminal, $c = \sqrt{D/\tau}$ the wavefront speed, τ the relaxation time, D the diffusion coefficient, and $u(\cdot)$ the step function.

The delay introduced by this block can be derived as

$$D_{H_2}(f) = -d\phi_{H_2}/df. \quad (8)$$

3.3. Postsynaptic element

In the postsynaptic element we model the fact that a chemical signal associated to the concentration of neurotransmitters released causes a binding of a percentage of the neurotransmitters with receptors. More specifically, two types of receptors are considered:

- *ionotropic* where the binding between neurotransmitters and receptors is direct, quickly leading to opening of ion channels;
- *metabotropic* where the binding activates a chain of reactions which slowly causes the opening of several ion channels placed on the postsynaptic membrane [5–7].

In order to fully characterize the postsynaptic element, we need to analyze the receptor–ligand binding process. An ion channel can be modeled as in either one of two states: *open* or *closed*.[5] We call α and β the two kinetic constants of the two-directions reaction. Accordingly, by using the Markov theory of flows balancing between the two states open and closed, the following kinetic scheme holds [8]:

$$R + T \overset{\alpha,\beta}{\longleftrightarrow} TR^* \quad (9)$$

where R and T represent the receptor and neurotransmitters concentration respectively, and TR^* represents the binding concentration. We also assume that the total postsynaptic receptor concentration $[A]$ is constant, which means that $[R] + [TR^*] = [A]$.

Then, we define r as the fraction of bound receptors, i.e. $r = \frac{[TR^*]}{[A]}$.

According to a first order kinetic scheme [8], the following equation can be written

$$dr/dt = \alpha T'(t)(1 - r(t)) - \beta r(t). \quad (10)$$

Observe that this equation is general and can be used to describe the functioning of the postsynaptic element both in cases of ionotropic and metabotropic receptors.

Accordingly, the gain associated to the channel and the postsynaptic elements can be written by solving Eq. (10) assuming that $T(t)$ is described as in Eq. (2), as follows:

$$H_3(f) = \frac{\frac{r_0+\tau_r}{1+j2\pi f(r_0+\tau_r)}\left(r_0 e^{\frac{t_0-t_1}{r_0+\tau_r}} - 1\right) + \frac{r(t_1)}{\beta+j2\pi f}}{(t_1 - t_0)\mathrm{sinc}(f(t_1 - t_0))e^{-j2\pi f(t_1-t_0)}} \quad (11)$$

where t_0 has been assumed equal to 0, r_0 is the value of the fraction of bound receptors at t_0, r_1 is the value of the fraction of bound receptors at t_1, and $\tau_r = \frac{1}{\alpha T_M+\beta}$. The normalized gain can be straightforwardly obtained from Eq. (11). The delay associated to this postsynaptic element will consequently be

$$D_{H_3}(f) = -d\phi_{H_3}/df. \quad (12)$$

[5] In case a multitude of intermediate states between open and closed are considered, it has been proved that the additional complexity of the binding model is not paid in terms of a significant increase in the precision of the model computation with respect to a two state model [7].

3.4. Ion current generator

When receptor–ligand binding causes directly an ion channel opening, the total conductance through all channels can be written as $G(t) = g_{syn}r(t)$ where g_{syn} is the maximum synaptic conductance.

Concluding, the synaptic current resulting from this process can be defined as [5,6]:

$$I_{syn}(t) = g_{syn}r(t)(E_r - V_{syn}(t)) \quad (13)$$

where $V_{syn}(t)$ is the membrane potential of the postsynaptic cell, i.e. $V_{syn}(t) = I_{syn}(t)Z_{syn}$, and E_r is the synaptic resting potential. Observe that, typically, the membrane potential is negligible as compared to the synaptic resting potential. This can be seen in Fig. 3 where the synaptic current behavior is shown both in the exact expression given in Eq. (13) and in the simplified case where the membrane potential is neglected and the current is approximated as

$$I_{syn}(t) \approx 0.5 \cdot g_{syn}r(t)E_r. \quad (14)$$

Looking at Fig. 3 it can be seen that the approximate expression well fits the real behavior while highly simplifying the reasoning. Accordingly, the normalized gain of this block, $H_4(f)$, which can be obtained from the simplified expression in Eq. (14), is unitary and the delay introduced, $D_{H_4}(f)$, is zero because the phase is $\Phi_4(f) = 0$ if $E_r \geq 0$ or $\Phi_4(f) = \pi$ if $E_r < 0$.

3.5. Membrane potential generator

This block models the process according to which the synaptic current is transduced into the membrane potential. In this section we discuss the mechanism of this transduction and how the generated signal is propagated through the neuron. We here introduce a realistic model which considers the possibility to have interactions among a pair of neurons while also having external stimuli applied to the dendrites of the neuron. More specifically, we consider that the stimuli occurring at the dendrites can be either excitatory or inhibitory. Excitatory stimuli are due to a depolarization of the cellular membrane, that is, when the membrane potential becomes more positive. Inhibitory stimuli, instead, are due to an hyperpolarization of the cellular membrane, that is, when the membrane potential becomes more negative.

In order to describe in detail the spatio-temporal pattern of stimuli applied to multiple regions of a neuron, as in real neurons, we used the Rall model proposed in [21]. The latter accounts for the effects of signal propagation through dendritic trees when assuming that different excitatory and inhibitory stimuli can be applied at various locations of the dendritic tree, simultaneously or not. The branched dendritic tree is modeled as an equivalent cable of passive uniform membrane. The distribution of the membrane potential along the length of each branch follows the cable equation and the description is accurate in the hypothesis that the branch diameters satisfy a specific relationship, i.e. the sum of the power 3/2 of the children branches' diameters is equal to the power 3/2 of the parent branch diameter. If this relationship is satisfied, it has been demonstrated that a model based on the finite

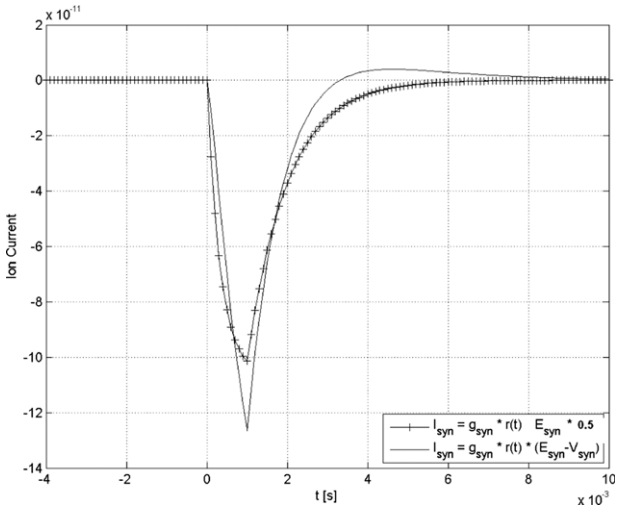

Fig. 3. Synaptic current.

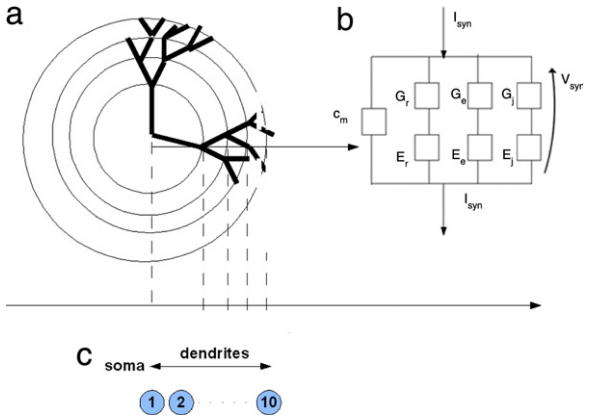

Fig. 4. Compartmental model.

length cable can be used to represent ideal dendritic trees; however, it was also shown that considering multiple *compartments* in the cable provides a better and more accurate approximation [21]. Typically, in order to achieve a good tradeoff between fitting realistic data and reducing the computational complexity of the model, it was shown that a compartmental model with 10 compartments along the cable between the soma (hereafter identified as Compartment 1), and the end of the dendritic tree (with branches identified as Compartments numbered from 2 to 10), provides a very good approximation. Synaptic excitation and inhibition are assumed to occur in any of the individual compartments to mimic the stimuli occurring on a neuron at various spatial and temporal locations.

The reference model is depicted in Fig. 4. More specifically, in Fig. 4(a) we show an example of dendritic tree; in Fig. 4(b) we show the membrane equivalent circuit for each compartment; in Fig. 4(c) we show the compartmental model composed of 10 compartments going from the soma (Compartment 1) to the end of the dendritic tree (Compartments $2 \cdots 10$).

The membrane equivalent circuit for each compartment shown in Fig. 4(b) can be represented as an equivalent RC parallel circuit driven by a current I_{syn} [10]. This current can be split into 4 components: (i) I_R that flows through the linear conductance G_r, which accounts for the resistive effects of the membrane and is related to E_r which is the resting electromotive force modeling the membrane resting potential; (ii) I_C that charges the capacitor C_m modeling the capacitive effects of the membrane; (iii) I_e that accounts for the current due to the excitatory stimuli which can occur on the specific compartment and is represented through the electromotive force E_e and the related conductance $G_e = \frac{1}{R_e}$; (iv) I_j that models the current due to the inhibitory stimuli which can occur in the specific compartment and is represented through the electromotive force E_j and the related conductance is $G_j = \frac{1}{R_j}$.

Observe that G_e and G_j are roughly proportional to the number of excitatory and inhibitory events that occur at the compartment. Usually E_r and E_j are negative and around -80 mV, while E_e is close to zero [8].

By using the model proposed in [21], any i-th compartment can be described as a system of ordinary linear first-order differential equations in the form:

$$\begin{cases} \dfrac{dV_{syn,i}}{dt} = \displaystyle\sum_{h=1}^{10} \mu_{i,h} V_{syn,h} + f_i \\ f_i = (\varepsilon_i + \beta_i \gamma_i + \chi_i)/\tau_i \\ \mu_{h,h} = -\dfrac{1 + \varepsilon_h + \gamma_h}{\tau_h} - \displaystyle\sum_{j \neq h} \mu_{h,j} \\ \mu_{h,j} = \dfrac{g_{h,j}}{c_h} = \dfrac{g_{j,h}}{c_i},\ h \neq j. \end{cases} \tag{15}$$

In the above set of equations, for the i-th compartment, the relevant parameters are defined as follows:

- $\varepsilon_i = [G_e/G_r]_i$;
- $\gamma_i = [G_j/G_r]_i$;
- $\tau_i = [C_m/G_r]_i$;
- $\beta_i = \left[\frac{E_j - E_r}{E_e - E_r}\right]_i$;
- $\chi_i = \left[\frac{I_{syn}/G_r}{E_e - E_r}\right]_i$.

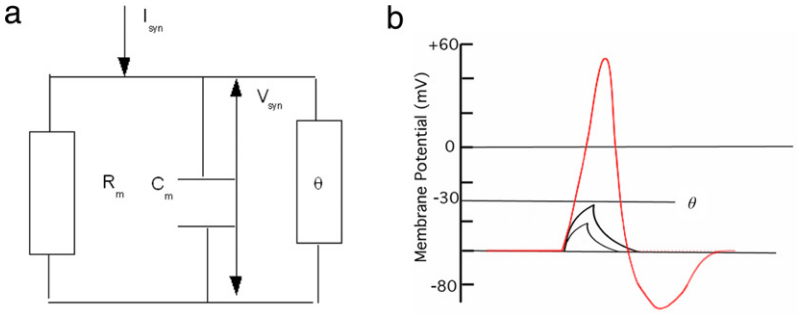

Fig. 5. (a) Leaky Integrate and Fire (LIF) model and (b) action potential threshold mechanism.

The synaptic membrane potential at the soma, $V_{Syn,1}$, also identifies the value of the synaptic voltage at the end of the backward dendritic tree.

At the soma (i.e., Compartment 1) the compartment equivalent circuit is slightly different from the other compartments. In fact, the model will be the more general Leaky Integrate and Fire (LIF) one [10] shown in Fig. 5. Observe that the LIF model is not a simple RC circuit, because a threshold mechanism is used. More specifically, when the voltage across the capacitor C_m reaches a threshold value denoted as θ, a spike (i.e. the action potential) is generated and is propagated through the axon. If the threshold is not reached, the action potential cannot be generated.

Thus, using the results of the previous subsections, we could appropriately determine the incoming voltage V_{syn} to be applied at the presynaptic element so that the action potential can be generated at the output of the membrane potential generator block.

The gain function of this block can be written as:

$$H_5(f) = \frac{V_{syn,1}(f)}{I_{syn}(f)} \tag{16}$$

and the delay, $D_{H_5}(f)$, can be calculated as

$$D_{H_5}(f) = -\frac{d\Phi_5(f)}{df}. \tag{17}$$

3.6. Axon

When the action potential is generated as a consequence of the threshold achievement in the membrane potential generator block, it propagates along the axon. Let us remind that the myelin sheath is occasionally interrupted at Ranvier nodes. At these locations, the action potential is regenerated so that it does not come at the axon terminal button too attenuated; in fact, in that case, it could not stimulate any synaptic communication. Accordingly, the axon can be modeled through a block which introduces a unit gain $H_6(f) = 1$ and a constant delay $D_{H_6}(f) = \Psi$.

4. Analysis

In this section we discuss the gains and delays introduced by the different blocks illustrated in the previous sections.

In Fig. 6(b) we show the normalized gain in Eq. (6) achieved by the channel (i.e. the synaptic cleft). Observe that the gain increases as a function of the frequency. More specifically, in [0.1, 10] Hz the neurotransmitter concentration increases according to a parabolic behavior. Then, in [10, 1000] Hz neurotransmitters' concentration remains almost constant and then it starts increasing again for higher values of the frequency.

Concerning the delay introduced by the channel and illustrated in Eq. (8) as shown in Fig. 7, in the range [0.1, 10] Hz the block does introduce a constant delay of less than 5 ns. Then, the delay introduced decreases rapidly and for higher frequencies starts increasing slowly again.

The normalized gain of the channel and postsynaptic elements as in Eq. (11) exhibits a high pass filter behavior, as shown in Fig. 6(b). Concerning the delay contribution in Eq. (12), observe in Fig. 7 that the contribution to the delay due to the postsynaptic element and the channel is in between about 6 and 12 ms; so, the block that introduces the higher delay is the postsynaptic one.

Let us now discuss on the membrane potential generator block. Preliminarily, we investigate on the effect of changing the locations where the input stimuli apply in the compartmental model. In Fig. 8 we assume a four-compartment model[6] and represent the associated normalized gain as a function of the input position. Varying the input position from the soma to the farthest compartment, the normalized gain decreases as the distance from the soma increases.

As already said the voltage across the capacitor C_m has to be at least equal to θ to make the action potential to be generated. Accordingly, in order to foster the action potential propagation from the input of the presynaptic element to the axon terminal button, it is necessary that the normalized gain between the voltage across the capacitor and the initial action potential is around $\frac{\theta}{V_{AP}}$ where V_{AP} is the action potential.

In Fig. 6(a) we show the behavior of the membrane potential as a function of the frequency at the input of the presynaptic element of the next neuron. Observe that the behavior can be assimilated to a band pass filter with a useful bandwidth of about 3 kHz. The overall delay in the corresponding frequency interval, as shown in Fig. 7(c), is in the range [1, 6] ms and is given by the sum of the delays introduced by the previous blocks. Finally, concerning the

[6] We have considered four compartments only, as this assumption provides a good trade-off in terms of complexity of the model and accuracy of the results.

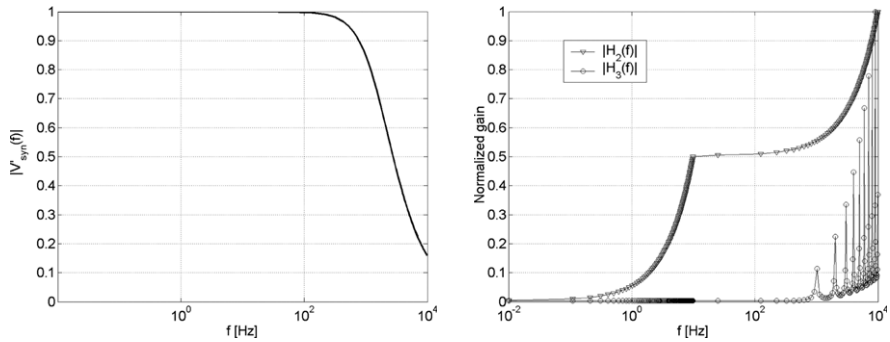

(a) $|V'_{syn}(f)|$. (b) $|H_2(f)|$, $|H_3(f)|$.

Fig. 6. (a) Action potential at the input of a presynaptic element and (b) normalized gain for $|H_2(f)|$ with $d_{Cleft} = 20$ nm $D = 10^{-6}$ m^2 s^{-1} $\tau = 1$ ns, and $|H_3(f)|$ with $\alpha = 2$ ms^{-1} mM^{-1} $\beta = 1$ ms^{-1} $r_0 = 10^{-7}$.

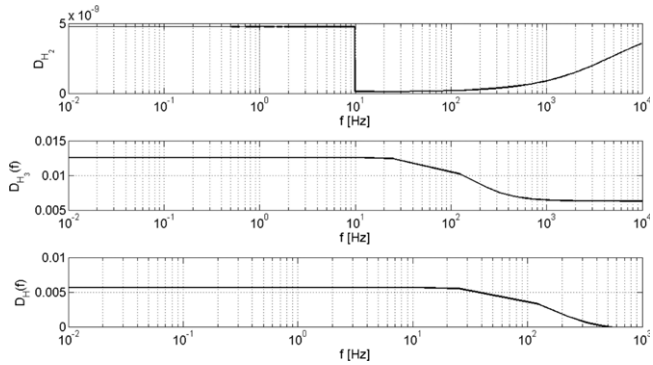

Fig. 7. Delay introduced by (a) channel ($D_2(f)$) (b) the postsynaptic element ($D_3(f)$) (c) delay introduced by the sequence of the first four blocks.

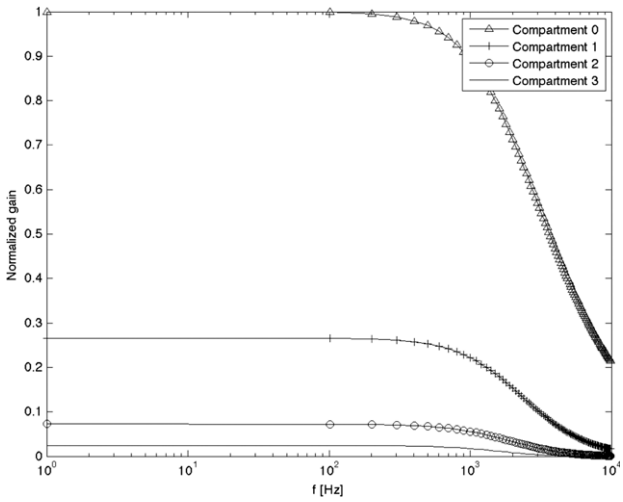

Fig. 8. $|H_5(f)|$ as a function of the applied input position, with $G_j = 0$ S, $G_e = 10^{-3}$ S, $G_r = 2 \cdot 10^{-4}$ S, $E_e = 0$ mV, $E_j = -77$ mV and $E_r = -70$ mV.

propagation in the axon which implies a regeneration in the action potential, the normalized gain can be considered unvaried but the delay is increased of the amount of time needed to regenerate the signal at each Ranvier node multiplied by the number of Ranvier nodes involved. Approximately, it is said that the propagation velocity of an electric pulse in the axon is around 100 m/s [8] which leads, in case for example of an axon length of 1 m (e.g. for the ischiatic nerve), to an additional delay of about 10 ms. Accordingly, the overall delay for the propagation of an

impulse between two neurons is in the range [11, 16] ms. The useful frequency bandwidth where it is possible for a nanomachine to effectively communicate with a neuron is around [0, 3000] Hz.

5. Conclusions

In this paper we have introduced a system description of a molecular neuronal model for nanomachine-to-neuron signal propagation in biological networks. The proposed solution is aimed at allowing communication between neurons and nanomachines which, on their turn, could work together to set up more complex nanonetworks; such nanonetworks, in the next future, could recover propagation of nervous pulses in areas of the human body that are misfunctioning as a consequence, for example, of a neurological disease or an accident.

The overall communication has been modeled as a sequential chain of blocks, each of which has been characterized in terms of gain and delay as a function of the working frequency. The results obtained show that there is a range of frequencies where a nanomachine, structured according to the blocks identified above, could successfully communicate with a neuron by introducing a delay which is compatible with the human reaction time.

References

[1] I.F. Akyildiz, F. Brunetti, C. Blazquez, Nanonetworks: a new communication paradigm, Elsevier Computer Networks (2008).

[2] B. Atakan, O.B. Akan, Carbon nanotube-based nanoscale Ad Hoc networks, IEEE Communications Magazine (2010).

[3] D.J.P. Colquhoun, B. Sakmann, Action of crief pulses of glutamate on AMPA receptors in patches from different neurons of rat hippocampal slices, Journal on Physion 458 (1992).

[4] B. Davies, Integral Transforms and Their Applications, Springer ed., 2002.

[5] A. Destexhe, Z.F. Maien, T.J. Sejnowski, Syntesis of model for excitable membranes, synaptic transmission and neuromodulation using a common kinetic formalism, Journal on Computational Neuroscience 1 (1994).

[6] A. Destexhe, Z.F. Mainen, T.J. Sejnowski, An efficient method for computing synaptic conductances based on a kinetic model of receptor binding, Neural Computation 6 (1994).

[7] A. Destexhe, Z.F. Mainen, T.J. Sejnowski, Synaptic currents, neuromodulation and kinetic models, Handbook of Brain Theory and Neural Networks (1995).

[8] G.L. Fain, Molecular and Cellular Physiology of Neurons, Harward University Press, 1999.

[9] L. Galluccio, S. Palazzo, G.E. Santagati, Characterization of signal propagation in neuronal systems for nanomachine-to-neurons communications, in: Proceedings of IEEE International Workshop on Molecular and Nano Scale Communication, MoNaCom, Shangai, PRC, April 2011.

[10] R. Gerstner, L. Kistler, Spiking neuron models, in: Single Neurons, Populations, Plasticity, Cambridge University Press, 2002.

[11] M. Gregori, I.F. Akyildiz, A new nanonetwork architecture using Flagellated bacteria and catalytic nanomotors, IEEE JSAC (2010).

[12] S. Hiyama, Y. Moritani, T. Suda, R. Egashira, A. Enomoto, M. Moore, T. Nakano, Molecular communication, NSTI Nanotechnology Conference (2005).

[13] K. Jensen, J. Weldon, H. Garcia, A. Zettl, Nanotuberadio, NanoLetters (2007).

[14] J.M. Jornet, I.F. Akyildiz, Graphene-based nano-antennas for electromagnetic nanocommunications in the Terahertz band, EUCAP (2010).

[15] J.M. Jornet, I.F. Akyildiz, Channel capacity of electromagnetic nanonetworks in the Terahertz band, IEEE ICC (2010).

[16] J.M. Jornet, I.F. Akyildiz, Electromagnetic wireless nanosensor networks, Elsevier Nano Communication Networks Journal (2010).

[17] M. Moore, A. Enomoto, T. Nakano, R. Egashira, T. Suda, A. Kayasuga, H. Kojima, H. Sakakibara, K. Oiwa, A design of a molecular communication system for nanomachines using molecular motors, IEEE PerCom (2006).

[18] T. Nakano, T. Suda, M. Moore, R. Egashira, A. Enomoto, K. Arima, Molecular communication for nanomachines using intercellular calcium signaling, IEEE NANO (2005).

[19] L. Parcerisa Gin, I.F. Akyildiz, Molecular communication options for long range nanonetworks, Elsevier Computer Networks (2009).

[20] M. Pierobon, I.F. Akyildiz, A physical end-to-end model for molecular communication in nanonetworks, IEEE JSAC (2010).

[21] W. Rall, Distinguishing theoretical synaptic potentials computed for different soma-dendritic distributions of synaptic input, Journal on Neurophysiology 30 (1967).

[22] B. Thide', Electromagnetic field theory, second ed. Online Textbook http://www.plasma.uu.se/CED/Book/index.html.

[23] J. Weldon, K. Jensen, A. Zettl, Nanomechanical radio transmitter, Physica Status Solidi (2008).

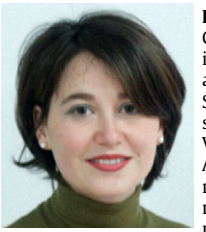

Laura Galluccio received her Ph.D. in Electrical, Computer and Telecommunications Engineering in March 2005. In 2005 she was a Visiting Scholar at the COMET Group, Columbia University, NY. Since 2002 she has been with the CNIT where she worked as a Research Fellow within the FIRB VICOM and NoE Satnex Projects. She is currently Assistant Professor at University of Catania. Her research interests include ad hoc and sensor networks, protocols and algorithms for wireless networks, network performance analysis and nanonetwork communications.

She serves in the EB of Wiley Wireless Communications and Mobile Computing and Elsevier Ad Hoc Networks Journal and is involved in the TPCs of many top level international conferences. She is also Guest Editor for the Special Issues of IEEE Wireless Communications Magazine on "Wireless communications at the nanoscale" and Elsevier Ad Hoc Network Journal on "Cross-Layer Deisgn in Ad Hoc and Sensor Networks".

Sergio Palazzo was born in Catania, Italy, on December 12, 1954. He received his degree in electrical engineering from the University of Catania in 1977. Until 1981, he was at ITALTEL, Milano, where he was involved in the design of operating systems for electronic exchanges. He then joined CREI, which is the center of the Politecnico di Milano for research on computer networks. Since 1987 he has been at the University of Catania, where is now a Full Professor of Telecommunications Networks. In 1994, he spent the summer at the International Computer Science Institute (ICSI), Berkeley, as a Senior Visitor. He is a recipient of the 2003 Visiting Erskine Fellowship by the University of Canterbury, Christchurch, New Zealand. Since 1992, he has been serving on the Technical Program Committee of INFOCOM, the IEEE Conference on Computer Communications. He has been the General Chair of some ACM conferences, including MobiHoc 2006 and MobiOpp 2010, and currently is a member of the MobiHoc Steering Committee. He has also been the TPC Co-Chair of the IFIP Networking 2011 conference. Moreover, in the recent past, he has been the Program Co-Chair of the 2005 International Tyrrhenian Workshop on Digital Communications, focused on "Distributed Cooperative Laboratories: Networking, Instrumentation, and Measurements", the General Vice Chair of the ACM MobiCom 2001 Conference, and the General Chair of the 2001 International Tyrrhenian Workshop on Digital Communications, focused on "Evolutionary Trends of the Internet". He currently serves the Editorial Board of the journal *Ad Hoc Networks*. In the recent past, he also was an Editor of *IEEE Wireless Communications Magazine* (formerly *IEEE Personal Communications Magazine*), *IEEE/ACM Transactions on Networking, IEEE Transactions on Mobile Computing, Computer Networks*, and *Wireless Communications and Mobile Computing*. He was a Guest Editor of Special Issues in the *IEEE Journal of Selected Areas in Communications* ("Intelligent

Techniques in High-Speed Networks"), in the *IEEE Personal Communications Magazine* ("Adapting to Network and Client Variability in Wireless Networks"), in the *Computer Networks* journal ("Broadband Satellite Systems: a Networking Perspective"), in the *EURASIP Journal on Wireless Communications and Networking* ("Ad Hoc Networks: Cross-Layer Issues", and "Opportunistic and Delay Tolerant Networks"). He also was the recipient of the 2002 Best Editor Award for the *Computer Networks* journal. His current research interests include mobile systems, wireless and satellite IP networks, intelligent techniques in network control, multimedia traffic modeling, and protocols for the next generation of the Internet.

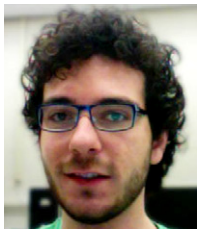

Enrico Santagati received his B.S. in Telecommunication Engineering from the University of Catania, Italy, in 2007. Currently, he is a M.S. student in Telecommunication Engineering at the University of Catania and his research interests include nanomachine communications, ultrasonic communications and green networking.